# Experiments on the synthesis of superheavy nuclei $^{284}$Fl and $^{285}$Fl in the $^{239,240}$Pu + $^{48}$Ca reactions

V. K. Utyonkov,[1,*] N. T. Brewer,[2] Yu. Ts. Oganessian,[1] K. P. Rykaczewski,[2] F. Sh. Abdullin,[1] S. N. Dmitriev,[1] R. K. Grzywacz,[2,3] M. G. Itkis,[1] K. Miernik,[2,4] A. N. Polyakov,[1] J. B. Roberto,[5] R. N. Sagaidak,[1] I. V. Shirokovsky,[1] M. V. Shumeiko,[1] Yu. S. Tsyganov,[1] A. A. Voinov,[1] V. G. Subbotin,[1] A. M. Sukhov,[1] A. V. Sabel'nikov,[1] G. K. Vostokin,[1] J. H. Hamilton,[6] M. A. Stoyer,[7] and S. Y. Strauss[8]

[1]*Flerov Laboratory of Nuclear Reactions, Joint Institute for Nuclear Research, RU-141980 Dubna, Russian Federation*
[2]*Physics Division, Oak Ridge National Laboratory, Oak Ridge, Tennessee 37831, USA*
[3]*Department of Physics and Astronomy, University of Tennessee, Knoxville, Tennessee 37996, USA*
[4]*Faculty of Physics, University of Warsaw, PL-02-093 Warsaw, Poland*
[5]*Science and Technology Partnerships Directorate, Oak Ridge National Laboratory, Oak Ridge, Tennessee 37831, USA*
[6]*Department of Physics and Astronomy, Vanderbilt University, Nashville, Tennessee 37235, USA*
[7]*Nuclear and Chemical Sciences Division, Lawrence Livermore National Laboratory, Livermore, California 94551, USA*
[8]*Department of Physics, University of Notre Dame, Notre Dame, Indiana 46566, USA*

(Received 22 July 2015; published 15 September 2015)

Irradiations of $^{239}$Pu and $^{240}$Pu targets with $^{48}$Ca beams aimed at the synthesis of $Z = 114$ flerovium isotopes were performed at the Dubna Gas Filled Recoil Separator. A new spontaneously fissioning (SF) isotope $^{284}$Fl was produced for the first time in the $^{240}$Pu + $^{48}$Ca (250 MeV) and $^{239}$Pu + $^{48}$Ca (245 MeV) reactions. The cross section of the $^{239}$Pu($^{48}$Ca,$3n$)$^{284}$Fl reaction channel was about 20 times lower than predicted by theoretical models and about 50 times lower than the maximum fusion-evaporation cross section for the $3n$ and $4n$ channels measured in the $^{244}$Pu + $^{48}$Ca reaction. In the $^{240}$Pu + $^{48}$Ca experiment, performed at 245 MeV in order to maximize the $3n$-evaporation channel, three decay chains of $^{285}$Fl were detected. The $\alpha$-decay energy of $^{285}$Fl was measured for the first time and decay properties of its descendants $^{281}$Cn, $^{277}$Ds, $^{273}$Hs, $^{269}$Sg, and $^{265}$Rf were determined with higher accuracy. The assignment of SF events observed during the irradiation of the $^{240}$Pu target with a 250 MeV $^{48}$Ca beam to $^{284}$Fl decay is presented and discussed. The cross sections at both $^{48}$Ca energies are similar and exceed that observed in the reaction with the lighter isotope $^{239}$Pu by a factor of 10. The decay properties of the synthesized nuclei and their production cross sections indicate a rapid decrease of stability of superheavy nuclei as the neutron number decreases from the predicted magic neutron number $N = 184$.

DOI: 10.1103/PhysRevC.92.034609 PACS number(s): 27.90.+b, 25.70.−z, 23.60.+e, 25.85.Ca

## I. INTRODUCTION

Twenty-five even-$Z$ and twenty-nine odd-$Z$ nuclides originating from superheavy nuclei (SHN) $^{281–285}$Cn, $^{282–286}$113, $^{285–289}$Fl, $^{287–290}$115, $^{290–293}$Lv, $^{293,294}$117, and $^{294}$118 at the hot fusion island have been synthesized in fusion-evaporation reactions using $^{48}$Ca beams and actinide targets from $Z = 92$, $^{238}$U to $Z = 98$, $^{249}$Cf during the last 15 years (see, e.g., review [1], and references therein). These studies were carried out in several laboratories, with the first successful experiments performed at the Flerov Laboratory for Nuclear Reactions (FLNR) at the Joint Institute for Nuclear Research (JINR) using the Dubna Gas Filled Recoil Separator (DGFRS). The results obtained at Dubna were confirmed and in some cases extended in experiments performed at GSI Darmstadt using the separators SHIP and TASCA, and at LBNL's separator BGS [1]. Decay properties of these nuclides were determined from more than 220 decay chains. Results from the overwhelming majority of experiments performed in different laboratories are in close agreement.

Several attempts have been undertaken to expand the region of SHN. The synthesis of elements 119 and 120 was attempted by using target nuclei ranging from $^{238}$U to $^{249}$Cf with projectiles heavier than $^{48}$Ca, from $^{50}$Ti to $^{64}$Ni. However, no decay chains of parent nuclei or their descendants were observed in these experiments. The upper cross-section limits were set at 0.07–1.1 pb depending on the reaction studied [2–5].

At present, the region of known SHN with $Z \leqslant 118$ and their $\alpha$-decay descendants forms a relatively narrow "ridge" in the nuclear landscape, with $N$-$Z$ values within a range of 56 to 61. Up to five isotopes of a given element with $Z \geqslant 112$ were synthesized. Their decay properties demonstrate the increasing influence of the neutron magic number predicted to be $N = 184$ by most theoretical approaches. Further investigations of superheavy nuclei performed with advanced detection setups can reveal interesting features of their structure also predicted by theory, e.g., a transition from oblate to prolate shapes, or from superdeformed to low-deformed prolate shapes, or even coexistence of shapes in the transition region between shells at $N = 162$ and $N = 184$ (see, e.g., Refs. [6–8]). Such effects could be at least partially revealed by observations of fine structure in $\alpha$ decay and detection of isomeric states. The $\alpha$-particle spectra of odd-$Z$ SHN are in general rather complex, but several $\alpha$-particle energies were also observed for some even-$Z$, odd-$N$ isotopes ($^{283}$Cn, $^{289}$Fl, and $^{291}$Lv). So far, no isomeric states have been identified within the hot fusion island (see, e.g., Ref. [1]). However, the observations of excited states in superheavy nuclei also provide important guidance for nuclear theory. The results of the first attempt aimed at the measurement of X-rays and $\gamma$ rays in coincidence with $\alpha$

*utyonkov@sungns.jinr.ru

 

particles were presented in Ref. [9]. In these studies, several $\alpha$-$\gamma$ coincidences for $^{280}$Rg and $^{276}$Mt were observed, and the first experimental insights on the decay schemes of $^{276}$Mt and $^{272}$Bh were presented. These experiments demonstrated the prospects for investigating the nuclear structure of SHN [10].

At the same time, in order to more fully understand the role of shell stabilization in this region, it is essential to considerably extend the area of synthesized SHN. Production and measurement of heavier isotopes of the known SHN could trace the pattern of increased stability approaching the proposed magic number $N = 184$. With available actinide targets and $^{48}$Ca projectile combinations, more neutron-rich isotopes with $Z \leqslant 117$ could be produced in the $2n$-evaporation channel of the reactions $^{249}$Bk + $^{48}$Ca $\rightarrow$ $^{295}$117 and $^{248}$Cm + $^{48}$Ca $\rightarrow$ $^{294}$Lv with predicted cross sections of about 0.3–0.4 pb [11,12]. The irradiation of a mixed-Cf target containing about 36% $^{251}$Cf with $^{48}$Ca beams may lead to the identification of two new isotopes of $Z = 118$: $^{295}$118 and $^{296}$118 [13]. Reaching the area of even-more-neutron-rich isotopes might be possible with the use of beams of nuclei with larger neutron excess than $^{48}$Ca. However, the intensity of radioactive-ion beams at the most advanced accelerators and even at those being designed is too low for performing such experiments.

Considering only the available target-projectile combinations, expanding the hot fusion island towards more neutron-deficient SHN seems to be easier. Several target nuclei could be used in these studies, e.g., $^{241}$Am, $^{239,240}$Pu, $^{233–236}$U, or $^{232}$Th. The comparison of decay properties of nuclei at the western border of SHN with those of nuclides located closer to neutron shells at $N = 162$ and $N = 184$ could clarify the scale of the stabilizing effect of these shells. One can note that $\alpha$ decay was observed for 35 nuclei, with $N = 162$ to 172, but only two of them are even-even nuclei ($^{270}$Hs and $^{286}$Fl). There were 15 nuclei, with $N = 160$ to 170, for which spontaneous fission (SF) was registered (electron capture followed by SF of daughter Rf isotopes is not excluded for some of $^{266–270}$Db nuclei), and there are only three even-even cases among these ($^{262}$No, $^{266}$Sg, and $^{282}$Cn). Thus, measurements of $\alpha$-decay and SF properties of even-even nuclei in this region would be important for tracing the decreasing influence of neutron-shell effects as $N$ increases above $N = 162$. In addition, the $\alpha$-decay chains of some odd-$N$ and/or odd-$Z$ nuclei, e.g., $^{285}$115 or $^{283}$Fl, could reach known nuclei at $N \approx 162$, connecting the hot fusion island to the "nuclear mainland." However, in accordance with theoretical predictions, the decrease of fission barriers for new, more-neutron-deficient SHN could lead to a drop in production cross section like those that were already observed for the $^{233}$U + $^{48}$Ca ($\sigma_{xn} \leqslant 0.6$ pb [14]) and $^{237}$Np + $^{48}$Ca ($\sigma_{3n} = 0.9^{+1.6}_{-0.6}$ pb [15]) reactions.

In this work, we present the results of experiments on the synthesis of neutron-deficient Fl isotopes in the $^{239}$Pu + $^{48}$Ca and $^{240}$Pu + $^{48}$Ca fusion-evaporation reactions. These experiments have provided evidence for the SF decay of a new isotope, $^{284}$Fl, and new properties of the $^{285}$Fl decay chain.

## II. EXPERIMENT

The experiments were performed at the Dubna Gas-Filled Recoil Separator using the $^{48}$Ca beam accelerated at the U400 cyclotron of the Flerov Laboratory of Nuclear Reactions, JINR. The $^{48}$Ca ion beam beam was delivered to the target with a maximum intensity of 1.3 particle $\mu$A. The beam energy was determined with a systematic uncertainty of 1 MeV by a time-of-flight system placed in front of the DGFRS.

The target materials were provided by Oak Ridge National Laboratory (ORNL) ($^{240}$Pu, enrichment of 98.97%) and JINR ($^{239}$Pu and $^{240}$Pu, enrichment of 98.2% and 92%, respectively). The impurities in the $^{239}$Pu and $^{240}$Pu targets mainly consisted of $^{240}$Pu and $^{239}$Pu, respectively. The average thicknesses of the targets for the main isotopes were $0.50 \pm 0.05$ mg/cm$^2$ for $^{239}$Pu and $0.39 \pm 0.04$ mg/cm$^2$ for mixed ORNL/JINR $^{240}$Pu material in the ratio 1/5 (given uncertainties correspond to standard deviations of thicknesses measured for six sectors of each target). The targets were manufactured by depositing $PuO_2$ oxide onto 0.71–0.72 mg/cm$^2$ Ti foils. Each target had an area of 5.4 cm$^2$ in the shape of an arc segment with an angular extension of 60° and an average radius of 60 mm. The segments were mounted on a disk that was rotated at 1700 rpm such that the target was perpendicular to the direction of the incoming beam. In the course of the bombardment with the $^{48}$Ca beam, the target layers were systematically monitored by counting $\alpha$ particles from the decay of the target isotopes.

The laboratory-frame beam energies in the middle of the target layers, excitation energy ranges (with use of mass tables [16,17]), and beam doses for the experiments studied are summarized in Table I. For calculation of excitation-energy ranges of the resulting compound nuclei $^{287,288}$Fl, we applied the Monte Carlo method and took into account the beam-energy resolution, the small variation of the beam energy during irradiation, and the energy loss in the target.

Evaporation residues (ERs) recoiling from the target were separated in flight from $^{48}$Ca beam ions, scattered particles, and transfer-reaction products by the DGFRS. The transmission efficiency of the separator for $Z = 114$ nuclei was estimated to be about $35\% \pm 5\%$. Recoils passed through a time-of-flight (TOF) system and were implanted in the detectors. The TOF system consists of two multiwire proportional counters (MWPCs) placed at a distance of 65 mm between them. The detectors and MWPC are placed in pentane at a pressure of about 1.5 Torr. A 0.2 mg/cm$^2$ Mylar foil separates the detection system from the DGFRS volume, which is filled with hydrogen at a pressure of 1 Torr.

The array of Silicon detectors at the DGFRS final focus has been modified to increase the position resolution of recorded signals and subsequently reduce the probability of observing sequences of random events that mimic decay chains of implanted nuclei. The new detection system includes

TABLE I. Target, reaction-specific laboratory-frame beam energies in the middle of the target layers, corresponding excitation-energy intervals, and total beam doses for the given reactions.

| Target | $E_{\rm lab}$ (MeV) | $E^*$ (MeV) | Beam dose |
|---|---|---|---|
| $^{240}$Pu | 245 | 36.5–41.1 | $4.0 \times 10^{18}$ |
| $^{240}$Pu | 250 | 40.9–45.4 | $4.7 \times 10^{18}$ |
| $^{239}$Pu | 245 | 35.4–40.0 | $1.4 \times 10^{19}$ |

a 0.3-mm-thick double-sided silicon strip detector (DSSD) manufactured by Micron Semiconductor, Ltd. (model BB-17). This large DSSD has 1-mm-wide strips, 48 on the front side and 128 on the back side, creating 6144 1 $mm^2$ pixels in one silicon wafer. Such high pixilation helps to achieve superior position resolution for recoil-correlated decay sequences reducing potential random events. The recoil implantation counter was surrounded by six single Si detectors, MICRON model MSX-7200, each 500 microns thick and having an active area of 65 mm by 120 mm. Two pairs of these Si-box detectors were mounted at the DSSD long side, and two detectors were used to close the Si-box geometry, one at each short side. All Si counters had a minimum amount of supporting frame material. The active detection length for the DSSD escape events was extended about 120 mm, from the DSSD surface towards the separator. The DSSD was backed by the single Si-veto detector (MICRON MSX-62), of 0.5 mm thickness and 48 mm by 128 mm active size matching the respective BB-17 area. This veto counter was mounted in the frame identical to the BB-17 support about 3 mm from the back surface of the DSSD. The signals from all detectors were processed by using MESYTEC preamplifiers. This new Si-detector array was designed, assembled, commissioned off-line, and provided by Oak Ridge National Laboratory.

The detection efficiency of the implantation DSSD, for $\alpha$ particles with $E_\alpha \approx 10$ MeV emitted from the implanted nuclei, is about 52%. The inclusion of the side MSX-7200 detectors, as measured for $^{217}$Th $\alpha$ activity produced in a calibration reaction $^{nat}$Yb + $^{48}$Ca at the DGFRS, increases the position-averaged detection efficiency for full-energy $\alpha$ particles from the decays of implanted nuclei to 85%. In the $^{206}$Pb($^{48}$Ca,$2n$)$^{252}$No calibration experiments, 52% of the SF events of $^{252}$No were detected as two coincident fragments in the focal and side detectors, with an average measured total energy release of 172 MeV. The MSX-62 detector was mounted behind the DSSD for the detection and rejection of signals recorded simultaneously in the DSSD and veto counters. These signals are triggered by high-energy charged particles ($\alpha$, protons, etc., produced in direct reactions of projectiles with the DGFRS media) which can pass through the separator without being detected by the TOF system.

The output signals from the MESYTEC linear-logarithmic preamplifiers serving BB-17 DSSD as well as linear preamplifiers serving MSX-7200 and MSX-62 detectors were split into two branches. One of these branches was processed with analog electronics similar to those used in previous DGFRS experiments; see Ref. [18]. The analog electronics system was used to create a dedicated low-background detection scheme for the nuclei to be investigated. This detection scheme allows the beam to be switched off after a predefined event sequence. The beam interruption occurs after the detection of a recoil signal with the expected implantation energy for $Z = 114$ evaporation residues followed by an $\alpha$-like signal in the implantation detector with an energy of 9.8–11.5 MeV, in the same front and back strips, i.e., in the same 1 $mm^2$ DSSD pixel. The ER energy interval was chosen to be 6–16 MeV, the same as in previous DGFRS experiments using position-sensitive single-strip Si detectors. This interval includes the ER energies in the three decay chains of $^{285}$Fl (see next section), where the average value of 10.91 MeV with standard deviation of 1.43 MeV has been measured. The triggering ER-$\alpha$ time interval was set to 1 s. The beam-off interval was initially set to 1 min. In this time interval, if an $\alpha$ particle with $E_\alpha = 8.5$ to 11.5 MeV was registered in the same front strip as the ER signal, the beam-off interval was automatically extended to 5 min. During this five minute period, if other $\alpha$ particles with energies expected for heavy nuclei were observed, we could prolong the beam-off pause further. This dedicated detection scheme is necessary for the registration of sequential decays of the daughter nuclides under very-low-background conditions.

The second branch of split preamplifier signals was processed by using a digital electronics system based on XIA Pixie-16 modules provided by ORNL. Such a digital pulse processing system was developed and applied successfully in earlier experiments on short-lived charged particle emitters at the Recoil Mass Separator (RMS) of ORNL's Holifield Radioactive Ion Beam Facility [19,20]. A similar system, with signals split between analog and digital electronics, was used during the search for element $Z = 120$ at the SHIP separator at GSI Darmstadt [21]. For the experiments at the DGFRS, thirteen 16-channel Pixie-16 modules were assembled in one PXI crate to process all signals from the silicon array and recoil gas detectors. The amplitude and time of incoming single signals were processed on board, while for the signals recognized as pileups, within the range of about 0.3 to 10 $\mu$s, the digital images (traces) were recorded [22]. Such hybrid analysis, developed at the Digital Pulse Processing Laboratory at the University of Tennessee (Knoxville) and commissioned during ORNL experiments, allows us to detect $\alpha$ particle and SF signals occurring even within submicrosecond time intervals after the implanted recoil. It simultaneously keeps the overall data rate and respective data acquisition dead time at a low level. Digital processing of DSSD signals at the DGFRS resulted in relatively low energy thresholds, of about 90 keV for the 48-mm-long back strips and about 500 keV for the 128-mm-long front strips. The use of custom-designed linear-logarithmic MESYTEC preamplifiers matching the Pixie-16 ADC range, pioneered in experiments using heavy-ion fragmentation [23], allowed us to detect low-energy deposits of $\alpha$ particles and high-energy SF events within the same single-input channel.

The full width at half maximum (FWHM) energy resolution of the implantation detector was 34 to 78 keV for back strips (55 to 83 keV for front strips), while the summed signals recorded by the side and implantation detectors had an energy resolution of 147 to 263 keV. Other experimental conditions, including the method of calibration of the detectors, were the same as in previous DGFRS experiments (see Ref. [1], and references therein).

## III. RESULTS

According to excitation functions measured in the reactions of $^{48}$Ca with target nuclei $^{238}$U–$^{249}$Cf (see Ref. [1], and references therein), the maximum of the cross section of the fusion-evaporation reaction $^{240}$Pu + $^{48}$Ca is expected at an excitation energy $E^*$ of the compound nucleus $^{288}$Fl of about 40 MeV. In the first experiment, performed at $^{48}$Ca

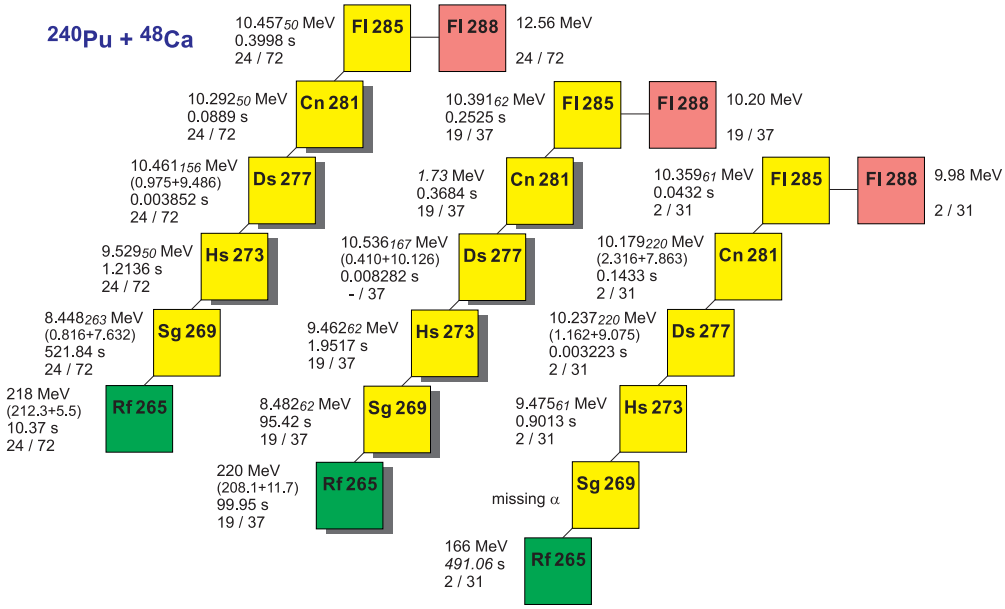


FIG. 1. (Color online) Decay properties of $^{285}$Fl and descendant nuclei observed in the $^{240}$Pu + $^{48}$Ca reaction at projectile energy of 245 MeV. The upper-right rows for each chain show ER (in pink) energies and strip numbers (front and back). The left rows provide energies, time intervals between events, and their strip numbers for $\alpha$ decay (in yellow) and SF (in green). Energies of summed signals are given in parentheses. Events marked with a shadow were registered during the beam-off periods. The $\alpha$-particle-energy errors are shown by smaller italic numbers. The time interval for a SF event following a "missing $\alpha$" was measured from the preceding registered event and is shown in italics.

energy $E_{\rm lab} = 245$ MeV (Table I), we observed three decay chains of $^{285}$Fl, the product of the $3n$-reaction channel (Fig. 1). This isotope was first registered in the $^{242}$Pu($^{48}$Ca,$5n$)$^{285}$Fl reaction at LBNL [24]. In their single-decay chain, the $\alpha$ particle of the parent nucleus escaped from the front of the five-sided detector box leaving the energy of 1.64 MeV in the implantation detector. Three further $\alpha$ decays of nuclei from $^{281}$Cn to $^{273}$Hs were detected with full energy by the front detector and one ($^{269}$Sg) simultaneously with the side one.

In all three decay chains observed in the present $^{240}$Pu + $^{48}$Ca reaction, the $\alpha$ particle of $^{285}$Fl was registered by the focal-plane detector with full energy which resulted in the first measurement of its energy $E_\alpha$. The decay times of nuclei $^{285}$Fl–$^{265}$Rf as well as $E_\alpha$ values of $^{281}$Cn–$^{269}$Sg in three chains are in good agreement with those measured in the $^{242}$Pu($^{48}$Ca,$5n$)$^{285}$Fl reaction [24]. Only the energies of $\alpha$ particles of $^{277}$Ds in the third chain and $^{273}$Hs in the second and third chains are somewhat lower than values measured in Ref. [24] (by about 0.33 and 0.12 MeV, respectively). With error bars of 0.22 and 0.04 MeV at $^{277}$Ds and 0.06 and 0.04 MeV at $^{273}$Hs these deviations are within statistical fluctuations.

During the 527 hour $^{240}$Pu + 245 MeV $^{48}$Ca experiment when the beam was on the target, the total number of sequences consisting of ER-like events with $E_{\rm ER} = 6$ to 16 MeV and $\alpha$-like events with $E_\alpha = 10.1$ to 10.7 MeV detected within 1.5 s in the same front and back strips of the focal-plane detector was only 57. In the first two decay chains of $^{285}$Fl shown in Fig. 1, the $\alpha$ decay of the parent nucleus switched the beam off. Three further $\alpha$ particles of $^{281}$Cn–$^{273}$Hs in the first case and four $\alpha$ particles of $^{281}$Cn–$^{269}$Sg and SF of $^{265}$Rf in the second chain were registered in the absence of beam-associated background. The total duration of beam-off intervals in this run was about 4.3 h. In the first chain, the beam-off pause was not manually prolonged and decays of $^{269}$Sg and $^{265}$Rf were registered when the beam was switched on. For beam-off $\alpha$ decays with $E_\alpha = 8$ to 11 MeV, the probability of their detection as random events in any crossing of strips within the period $\Delta t = 3$ min was about $1.3 \times 10^{-4}$ [25]. For beam on $\alpha$- and SF-like events with energies $E_\alpha = 8$ to 11 MeV and $E_{\rm SF} > 130$ MeV, respectively, and $\Delta t = 10$ min these values were $1.2 \times 10^{-2}$ and $1.3 \times 10^{-5}$, respectively. The decay of $^{281}$Cn in the second chain was registered by the focal-plane detector only with an energy of 1.7 MeV while the beam was stopped by a ER-$\alpha_1$ sequence. The probability of the random origin of an event with any energy in strips 19 and 37 within $\Delta t = 1$ s was less than $7 \times 10^{-3}$. In the third chain, the first $\alpha$ particle did not stop the beam, for an unknown reason. Two subsequent $\alpha$ decays were detected by both the focal-plane and side detectors and could not switch the beam off. Thus, all these events as well as the fourth $\alpha$ particle and the SF event were observed during the beam-on time interval. However, the probability of detection of random beam-on events with $E_\alpha = 8$ to 11 MeV within $\Delta t = 5$ s was $1.0 \times 10^{-4}$.

In the third chain, no $\alpha$ particles with $E_\alpha = 8$ to 11 MeV were found in strips 2 and 31 between decays attributed to $^{273}$Hs and $^{265}$Rf. This missing $\alpha$ event could be detected by the focal detector only with low energy release, but the probability of detection of similar random beam-on events within the time interval of 491 s is rather large, preventing the definite assignment of such an event to $^{269}$Sg. Missing this $\alpha$ particle

and incomplete detection of the energy of $^{281}$Cn in the second chain are in accordance with the 85% registration efficiency of the detectors. From the remaining 13 $\alpha$ particles, five decays were registered by both the implantation and side detectors which also corresponds to their detection efficiencies. In one of these events, the $\alpha$-particle energy of $^{277}$Ds absorbed by the focal detector was below the energy threshold, and the number of the front strip was not determined. However, the energy and corresponding strip number were registered at the back side of the detector.

The number of expected random $^{285}$Fl-like decay chains was calculated by multiplying the 57 ER-$\alpha_1$ chains by the corresponding probabilities of detection of different events ($\alpha$ and SF) assuming their random distribution over the focal-plane detector. Using rather broad energy intervals for $\alpha$ particles from $^{285}$Fl to $^{269}$Sg, the number of random correlations for any of the decay chains shown in Fig. 1 was calculated to be less than $10^{-15}$. The LLNL Monte Carlo random probability method estimates the number of these correlated decay chains due to random events to be less than $5 \times 10^{-17}$ [26]. These numbers of random correlations obtained by two different methods are upper estimates because the results of other experiments, energy systematics, and Geiger–Nuttall relationships were not taken into account. Thus, it is very unlikely that any of the decay chains could be attributed to a random correlation of unrelated events. The cross section of the $^{240}$Pu($^{48}$Ca,3$n$)$^{285}$Fl reaction at 245 MeV beam energy was measured to be $2.5^{+2.9}_{-1.4}$ pb. The given error bars include statistical uncertainties [25] at the 68% confidence level as well as systematic uncertainties in the beam dose ($\pm$7%), DGFRS's transmission, and registration efficiency of decay chains (>90%). For the effective target thickness in all experiments, we used the value of 0.4 mg/cm$^2$ for Pu assuming that the first part of the thick target just reduces the beam energy and the ERs produced in this layer would not be able to reach the detectors [27].

Identifying new isotopes by SF decay properties is difficult at best, because of long-lived SF backgrounds in the detector from prior experiments and the presence of SF isomers in near-target isotopes. Nevertheless, indications of a SHN with a SF decay branch can potentially be obtained by examining total fission energies and short ER-SF correlation times. In the same experiment, we found 21 recoil-(SF-like) chains with $E_R = 6$ to 16 MeV, $E_F > 130$ MeV, and upper time interval between events of $\Delta t = 100$ s. For 20 of these sequences, fission-like events were detected by the focal-plane detector only and R-F time intervals were randomly distributed between 0.53 and 97.4 s. These sequences indicate the level of total number of random ER-SF correlations, viz., $N_{ran} = 2 \times 10^{-3}$ for $\Delta t = 10$ ms, and are thus not considered further. One chain was detected simultaneously by the focal and side detectors but with a low total energy of fragments (131 MeV) and a relatively short decay time of 33 $\mu$s (see Fig. 2).

The energy spectrum of fission fragments observed in the experiments $^{243}$Am + $^{48}$Ca (28 ER-SF events), $^{242}$Pu + $^{48}$Ca (8 events), and $^{238}$U + $^{48}$Ca (1 event) [14,28,29], which we attributed to SF isomers of $^{240,242,244}$Am [30] because their decay times were comparable with half-lives of 1 and 14 ms, is shown in Fig. 2. Here open and gray histograms correspond to all SF events and those detected by both the focal and side detectors, respectively. The Gaussian fit of the spectrum of all data for isomers is shown by a smooth curve. The vertical dash-dotted line shows the energy interval corresponding to a shift from the middle value ($E = 157.1$ MeV) by more than two standard deviations ($\sigma = 12.3$ MeV). Thus, the probability of observing SF isomers with $E \geqslant 181.7$ MeV is less than 2.3%. Similar spectra for $^{252}$No produced in the $^{206}$Pb + $^{48}$Ca reaction and SHN with $Z = 109$ to 114 observed in previous

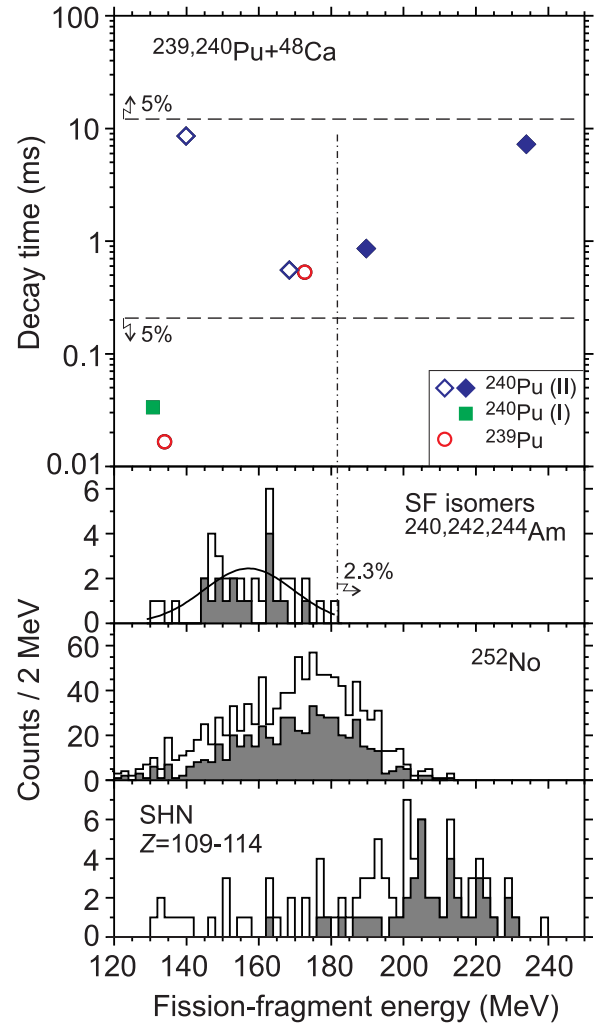


FIG. 2. (Color online) The top panel shows the decay time vs fission-fragment energy of recoil-SF events observed in the reactions of $^{48}$Ca with $^{239}$Pu (circles) and $^{240}$Pu at 245 MeV (square) and 250 MeV (diamond) projectile energies. Energies of SF events detected solely by the front detector or together with the side detector are shown by open and solid symbols, respectively. Horizontal lines correspond to 90% probability time interval for observation of decays with a half-life of 2.8 ms. The three bottom panels show the energy spectra of $^{240-244}$Am SF isomers, $^{252}$No, and SHN with $Z = 109$ to 114. Open and gray histograms correspond to all SF events and those detected by both the focal and side detectors, respectively. Gaussian fit of all data for isomers is shown by smooth curve. The vertical line shows the energy interval corresponding to a shift from the middle value for isomers by more than two standard deviations.

experiments are also shown in Fig. 2. All these spectra represent distributions of measured fragment energies which were not corrected for the pulse-height defect of the detectors, or for energy loss in the detectors' entrance windows, dead layers, and the pentane gas filling the detection system. One can note that, in agreement with empirical systematics of the mean total kinetic energies of fission fragments vs the parameter $Z^2/A^{1/3}$ (see, e.g., Refs. [14,31]), the centers of the energy spectra for fission isomers, $^{252}$No, and nuclei with $Z = 109$ to 114 gradually increase for the heavier nuclides.

The top part of Fig. 2 shows the distribution of decay times vs fission-fragment energies of recoil-SF events in the reactions of $^{48}$Ca with $^{239}$Pu (circle) and $^{240}$Pu at 245 MeV (square) and 250 MeV (diamond) projectile energies. Energies of SF events detected solely by the front detector or together with the side detector are shown by open and solid symbols, respectively. As one can see, the energy of the 131 MeV event is indistinguishable from the energies of events attributed to fission isomers.

In the second experiment, the energy of $^{48}$Ca was increased to 250 MeV for measurement of the excitation function of the $^{240}$Pu + $^{48}$Ca reaction and possible observation of the product of the $4n$-evaporation channel, the new lightest isotope $^{284}$Fl. From systematics of $\alpha$-decay properties and SF half-lives of the heavy nuclei with $Z = 112$ to 116 (see Figs. 5, 6 below), one could expect that SF would be the dominating decay mode for $^{284}$Fl. In this experiment, decay chains of $^{285}$Fl were not observed, which indicates a decrease of the cross section of the $3n$ channel at this $^{48}$Ca energy ($\sigma_{3n} \leqslant 1.3$ pb).

However, in this run, four ER-SF chains were found which are shown in Fig. 2. In addition, 27 recoil-fission (focal-plane-only events) were found with $E_R = 6$ to 16 MeV, $E_F > 130$ MeV, and $\Delta t = 100$ s, with a random distribution of R-F time intervals varying from 3.3 to 96.6 s; therefore, the total number of random ER-SF chains for $\Delta t = 10$ ms is $3 \times 10^{-3}$.

In Fig. 2 the energies and decay times for four ER-SF chains are shown by blue diamonds. In two cases, both fission fragments were registered by the focal and side detectors with rather large total energies (closed symbols) which differ from the average energy for SF isomers by 2.65 and 6.25 standard deviations. Thus, these events could originate from isomers with very low probabilities of $4 \times 10^{-3}$ and $2 \times 10^{-10}$, respectively. Taking into account this fact as well as the nonobservation of such ER-SF chains at 245 MeV $^{48}$Ca beam energy ($\sigma_{4n} \leqslant 1.7$ pb) and the agreement of these results with expectations for the behavior of the excitation function for the $4n$-reaction channel and from calculated and measured decay properties of even-even nuclei (see Fig. 5 below), the assignment of two high-energy SF events to $^{284}$Fl seems quite reasonable.

Therefore, we propose that the new isotope $^{284}$Fl, which undergoes SF with half-life $T_{1/2} = 2.8^{+5.1}_{-1.1}$ ms, was produced in the $^{240}$Pu($^{48}$Ca,$4n$) reaction with a cross section of $2.6^{+3.3}_{-1.7}$ pb (taking into account 52% probability for detection of both fission fragments). Decay properties of these chains are shown in Fig. 3.

For the given $T_{1/2}$ value, we estimated the range of decay times which could be observed for this nucleus with probability of 90%. The horizontal lines in Fig. 2 show the time limits which correspond to 5% probabilities for registration of shorter and longer lifetimes. As can be seen, two other ER-SF sequences where SF events were detected solely by the front detector with $E_{SF} = 140$ and 168 MeV in this experiment also could originate from $^{284}$Fl. Their deposited energies are within the interval where energies of fission fragments of SHN with $Z = 109$ to 114 were registered and decay times are within the 90% interval for detection of activity with $T_{1/2} = 2.8$ ms. Note that assignment of these events to $^{284}$Fl practically does not change its half-life ($T_{1/2} = 3.0^{+2.7}_{-1.0}$ ms) and production cross section ($\sigma_{4n} = 2.7^{+2.3}_{-1.3}$ pb) but is less certain due to lower SF energies which are also consistent with SF isomers.

The same nucleus $^{284}$Fl could be produced in the $3n$-evaporation channel of the reaction with the lighter Pu isotope, $^{239}$Pu + $^{48}$Ca, and its observation could make a cross-bombardment consistency check on the synthesis of the new Fl isotope. This experiment was performed at a $^{48}$Ca

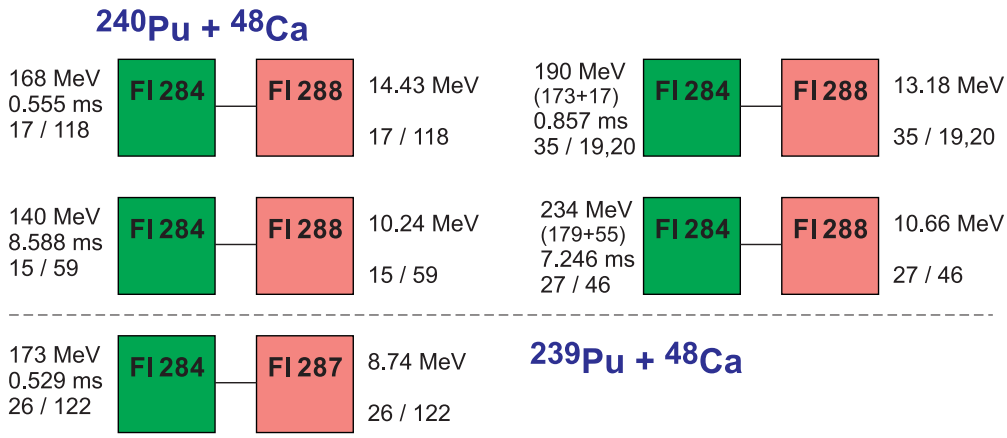


FIG. 3. (Color online) Decay properties of nuclei assigned to $^{284}$Fl observed in the $^{240}$Pu + $^{48}$Ca reaction (top) and $^{239}$Pu + $^{48}$Ca reaction (bottom), see text for details. The right rows for each chain show ER (in pink) energies and strip numbers (front and back). The left rows provide SF fragment (in green) energies, time intervals between events, and their strip numbers. The decay chain shown in the top-right corner was registered in two back strips.

energy which corresponds to expected maximum of the cross section of the $3n$-evaporation channel [32]. The experimental conditions are summarized in Table I.

In the $^{239}$Pu + $^{48}$Ca reaction, two short ER-SF chains with decay times of 0.53 ms and 17 $\mu$s were detected (see Figs. 2 and 3) as well as 30 another chains with $E_R = 6$ to 16 MeV, $E_F > 130$ MeV, and $\Delta t = 100$ s (again all these fission-like events were detected by the focal-plane detector only). As in the previous case, the number of random ER-SF chains for $\Delta t = 10$ ms was estimated to be $3 \times 10^{-3}$.

One of these events was detected by the focal-plane detector (solely) with a relatively high fragment energy (173 MeV) and decay time which conforms to a time interval where decays of 2.8 ms SF activity were detected in the $^{240}$Pu + $^{48}$Ca reaction. The energy of the $^{48}$Ca in the reaction with $^{239}$Pu was the same as in the $^{240}$Pu experiment where the $3n$-reaction channel was observed. This also corresponds to the predicted cross-section maximum of the $^{239}$Pu($^{48}$Ca,$3n$)$^{284}$Fl reaction [32]. Additionally, all of the decay chains given in Fig. 3 are similar. Based on these facts, one may assign this ER-SF chain to $^{284}$Fl. In that case, the average half-life of this isotope calculated for five decays would be equal to $T_{1/2} = 2.5^{+1.8}_{-0.8}$ ms. The production cross section was found to be $\sigma_{3n} = 0.23^{+0.59}_{-0.20}$ pb, which is lower by factor of ten than that for the reaction with $^{240}$Pu. An upper cross-section limit of 0.47 pb can be set if this decay does not originate from $^{284}$Fl.

The average decay properties of nuclei observed in this work and in Ref. [24] are given in Table II. We should note that, in spite of stated arguments which demonstrate that the 2.5-ms SF activity originates from $^{284}$Fl, this conclusion still requires additional confirmation, e.g., a detailed measurement of the excitation function of the $^{240}$Pu($^{48}$Ca,$4n$)$^{284}$Fl reaction or observation of $^{284}$Fl as $\alpha$-decay product of parent nucleus $^{288}$Lv. However, both of these measurements call for performing experiments with noticeably higher sensitivity.

As can be seen in Fig. 2, in addition to the 2.5 ms SF activity, two events were detected with obviously shorter decay times and relatively low energies of fission fragments. These low SF energies are more typical for light nuclei, e.g., fission isomers with $Z = 94$ or 95. For the aforementioned isomers $^{240,242,244}$Am, we observed a rather broad distribution of recoil energies $E_R = 2$ to 18 MeV. In this work, three more SF events with $E_R < 6$ MeV, $E_F = 115$, 126 ($E_{Ca} = 245$ MeV) and 174 MeV ($E_{Ca} = 250$ MeV) and decay times of 16.3, 16.9, and 53.3 $\mu$s, respectively, were found in the reaction with $^{240}$Pu. The apparent half-life for all five events is $19^{+14}_{-6}$ $\mu$s. Several SF isomers could contribute to this activity (e.g., $^{239,241}$Pu or $^{238}$Am). Based on the implantation energy and decay properties of events with an average half-life of 19 $\mu$s, it is most likely that they originate from nuclei different from $^{284}$Fl.

TABLE II. Decay properties of nuclei produced in this work and from Ref. [24].

| Nuclide | Decay mode | Half-life[a] | $E_\alpha$ (MeV)[b] | $Q_\alpha$ (MeV)[b] |
|---|---|---|---|---|
| $^{284}$Fl | SF | $2.5^{+1.8}_{-0.8}$ ms | | |
| $^{285}$Fl | $\alpha$ | $0.15^{+0.14}_{-0.05}$ s | $10.41 \pm 0.05$ | $10.56 \pm 0.05$ |
| $^{281}$Cn | $\alpha$ | $0.13^{+0.12}_{-0.04}$ s | $10.30 \pm 0.04$ | $10.45 \pm 0.04$ |
| $^{277}$Ds | $\alpha$ | $4.1^{+3.7}_{-1.3}$ ms | $10.55 \pm 0.04$ | $10.71 \pm 0.04$ |
| $^{273}$Hs | $\alpha$ | $0.76^{+0.71}_{-0.24}$ s | $9.53 \pm 0.04$ | $9.67 \pm 0.04$ |
| $^{269}$Sg | $\alpha$ | $3.1^{+3.7}_{-1.1}$ min | $8.50 \pm 0.06$ | $8.63 \pm 0.06$ |
| $^{265}$Rf | SF | $1.0^{+1.2}_{-0.3}$ min | | |

[a]Error bars correspond to 68%-confidence level.
[b]The energy uncertainties correspond to the data with the best energy resolution.

## IV. DISCUSSION

The unexpected result of this series of experiments is the observation of a strong decrease in the production cross section of the $^{239}$Pu + $^{48}$Ca reaction when compared with heavier target nuclei. The maximum measured fusion-evaporation cross sections for the reactions of $^{48}$Ca with isotopes $^{239,240,242,244}$Pu are shown in Fig. 4. The cross section of the $^{239}$Pu + $^{48}$Ca reaction decreases by a factor of about 50 in comparison with that for the reaction with the heavier isotope $^{244}$Pu. However, the value of about 3 pb was calculated in Ref. [33] for the $^{239}$Pu + $^{48}$Ca reaction at $E^* \approx 32.5$ MeV. According to recent predictions [32], the total ER cross section could reach about 4 pb at $E^* = 38$ to 39 MeV. Thus, the experimental value was found to be lower by factor of about 20 than the calculated value. Note that this model, describing the dynamics of capture of the interacting nuclei, formation of an excited compound nucleus, and its final cooling down by the emission of neutrons and $\gamma$ rays, reproduces reasonably accurately the measured cross-section values from all previously studied $^{48}$Ca-induced reactions with isotopes from $^{238}$U to $^{249}$Cf,

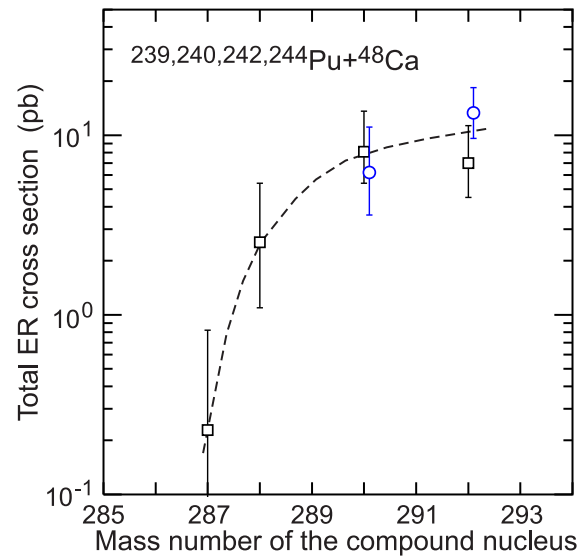


FIG. 4. (Color online) Maximum of the production cross sections of Fl isotopes in the $^{48}$Ca-induced reactions with targets shown in figure vs mass number of the compound nucleus. Data from DGFRS [14,34] are shown by squares as well as from BGS [24] ($^{290}$Fl) and TASCA [35] ($^{292}$Fl) by circles. Vertical error bars correspond to total uncertainties. The dashed line is drawn to guide the eye.

including $^{242,244}$Pu. Such a large deviation between theoretical and experimental data was not previously observed.

In this model [32], the capture cross section and fusion probability vary weakly over a rather large range of reactions leading to nuclei with $Z_{CN} = 112$ to 118. Indeed, capture cross sections are comparable for the $^{238}$U–$^{249}$Cf + $^{48}$Ca reactions [12], which are also in agreement with experimental data [36], and fusion probability slightly decreases for heavier target nuclei [12]. Thus, the resulting total ER cross section substantially depends on the survival probability of the excited compound nucleus which is determined mainly by the difference between the fission-barrier height and neutron binding energy of the nuclei for each step of sequential neutron emission. With decreasing number of neutrons, the fission barriers are predicted to be lower (see, e.g., Refs. [37,38]) while neutron-binding-energy values steadily (if neutron magic number is not crossed) increase undergoing 1 MeV fluctuations due to the odd-even effect for nuclei in this mass region [16,17,37,39,40]. Therefore, a large decrease of the production cross sections of neutron-deficient Fl isotopes and considerable difference with theoretical results [32], which were based on predicted fission barriers [37], would be caused by a stronger drop of fission barriers than expected. An approximate 1 MeV reduction in fission barrier height would be consistent with the experimental data (compare with Ref. [41]).

In accordance with reducing cross sections, the SF half-lives rapidly decrease for neutron-deficient even-even isotopes of Fl. This property of the nucleus is also governed by the fission barrier. The partial SF half-lives of nuclei with $N \geqslant 162$, produced in the $^{48}$Ca-induced reactions with $^{238}$U–$^{249}$Cf, together with the half-lives of SF nuclides with $N < 162$, are shown in Fig. 5. Here we show data for even-even isotopes only

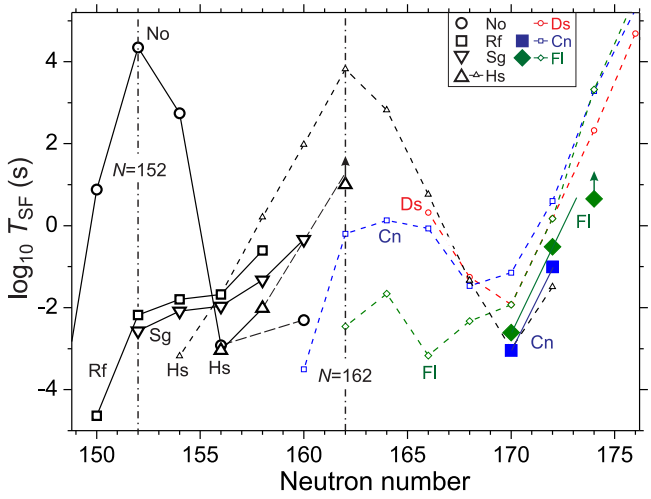


FIG. 5. (Color online) Common logarithm of experimental partial spontaneous fission half-life vs neutron number for even-even isotopes of elements with $Z = 102$ to 114 (data are from Refs. [1,44] and present work, larger symbols). Short-dashed lines connecting smaller symbols show the theoretical $T_{SF}$ values [42,43] for even-even $Z = 108$ to 114 isotopes. Long-dashed lines connect $T_{SF}$ values for isotopes $^{258,262}$No and $^{266,270}$Hs.

because their half-lives are not hindered by the influence of an unpaired neutron and/or proton. The influence of the $N = 152$ and 162 shells on the stability of nuclei against SF is clearly seen for isotopes of No and Rf-Hs, respectively. A similar stabilizing influence of the $N = 184$ shell seems apparent for Cn and Fl. These variations of $T_{SF}$ are in agreement with theoretical calculations within macroscopic-microscopic models [42,43], as well as with a recent self-consistent Skyrme-HFB approach [8].

For two even-even isotopes $^{282,284}$Cn with $N = 170$ and 172, the decrease of neutron number results in a steep drop of their SF partial half-life by two orders of magnitude. Similar decreases of stability against SF are observed also for the even-even isotopes $^{284,286}$Fl which have the same neutron numbers. For heavier even-even nuclei, SF was not detected due to a more considerable rise of stability with regard to SF compared with $\alpha$ decay when approaching the $N = 184$ proposed magic number [8,42,43] and thus only a lower $T_{SF}$ limit could be estimated. Therefore, both experimental observations—the decrease of production cross sections and the partial SF half-lives with respect to a lower number of neutrons—could indicate a lowering of fission barriers for neutron-deficient Cn and Fl isotopes and an approach to the limits of their stability. However, according to theoretical data [42] such a rapid decrease of $T_{SF}$ values for Cn and Fl isotopes might be followed by some stabilization of SF half-lives for Fl isotopes and even their growth for Cn isotopes due to influence of $N = 162$ shell (see Fig. 5).

It is interesting to note that $\alpha$-decay energies $Q_\alpha$ of nuclei synthesized in the $^{240}$Pu + $^{48}$Ca reaction also demonstrate a growing decrease of stability against $\alpha$ decay in comparison with their heavier neighbors. The systematics of $Q_\alpha$ values vs neutron number for the isotopes of elements 106–118 are shown in Fig. 6. For Fl isotopes with $N = 173$–175, the $\alpha$-decay energy gradually increases by about 0.1 MeV per neutron with approach to the neutron-deficient region. But for lighter isotopes $^{286}$Fl and $^{285}$Fl, $Q_\alpha$ value becomes larger by 0.2 MeV compared to the heavier Fl isotopes which results in an increased slope in systematics of the $\alpha$-decay energy. A similar break in $Q_\alpha$ lines is seen for isotopes of Cn and in element 113 as well.

As one could expect from the dependence of $T_{SF}$ vs neutron number for $^{282,284}$Cn and $^{286}$Fl isotopes as well as theoretical calculations [42] (Fig. 5), only spontaneous fission was observed for $^{284}$Fl. But its SF half-life is relatively large in comparison with the partial $\alpha$-decay half-life which might be estimated from extrapolation of $Q_\alpha$ systematics (Fig. 6) and the $T_\alpha$ vs $Q_\alpha$ relationship, e.g., from the Viola–Seaborg formula. From this one would expect about 20% $\alpha$-decay branch for $^{284}$Fl. Observation of this decay mode in future experiments would be important for final identification of $^{284}$Fl and registration of its descendant(s), presumably, the spontaneously fissioning $^{280}$Cn.

In summary, a series of experiments aimed at investigation of the neutron-deficient region of superheavy nuclei was performed with use of the $^{239}$Pu + $^{48}$Ca and $^{240}$Pu + $^{48}$Ca reactions. In the $^{240}$Pu + $^{48}$Ca reaction, three decay chains of $^{285}$Fl were observed. The $\alpha$-particle energy of $^{285}$Fl ($E_\alpha$ = 10.41 ± 0.05 MeV) was measured for the first time. The decay

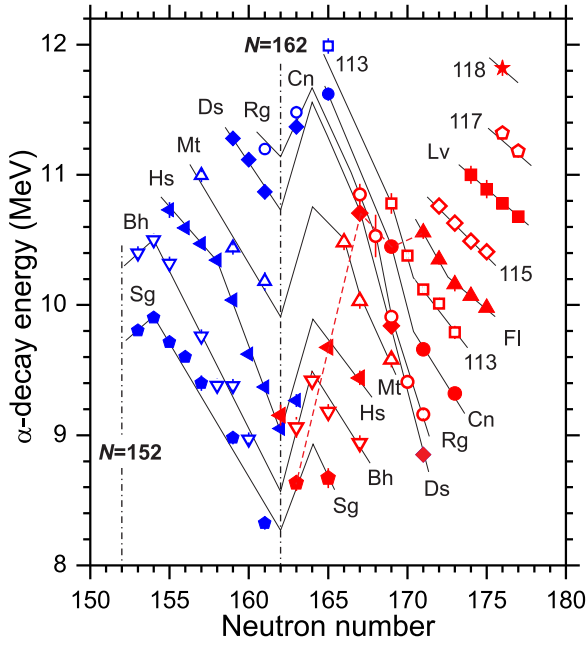


FIG. 6. (Color online) Measured $\alpha$-decay energy vs neutron number for the isotopes of elements 106–118. Solid and open symbols refer to even-$Z$ and odd-$Z$ nuclei, respectively; $Q_\alpha$ values for nuclei produced in the Ra-Cf + $^{48}$Ca reactions are shown in red; other data (blue symbols) are taken from Refs. [16,45]. The lines are drawn to guide the eye. Data from the current work are shown as symbols connected by dashed lines.

properties of isotopes $^{285}$Fl, $^{281}$Cn, $^{277}$Ds, $^{273}$Hs, $^{269}$Sg, and $^{265}$Rf were determined more precisely. The cross section of the $^{240}$Pu($^{48}$Ca,$3n$)$^{285}$Fl reaction for 245 MeV projectiles was measured to be $2.5^{+2.9}_{-1.4}$ pb, which exceeds that for $^{239}$Pu by a factor of ten but is two to four times lower than that for $^{244}$Pu.

Two ER-SF decay chains observed in the $^{240}$Pu + 250 MeV $^{48}$Ca reaction with high energy release of fission fragments ($E_{SF} = 190$ and 234 MeV) are assigned to the new spontaneously fissioning isotope $^{284}$Fl. Two more ER-SF events registered with lower energy values ($E_{SF} = 140$ and 168 MeV) could also originate from $^{284}$Fl (assignment to $^{240,242,244}$Am fission isomers is also not rejected). The cross section of the $^{240}$Pu($^{48}$Ca,$4n$)$^{284}$Fl reaction ($2.6^{+3.3}_{-1.7}$ pb) is similar to that for the $3n$-reaction channel.

In the $^{239}$Pu + $^{48}$Ca reaction, one ER-SF chain was observed with SF decay properties comparable with those registered for $^{284}$Fl in the reaction with $^{240}$Pu. The production cross section for this event, presumably the product of the $^{239}$Pu($^{48}$Ca,$3n$)$^{284}$Fl reaction, of 0.2 pb is 20 times lower than the theoretically predicted value and 50 times lower than maximum fusion-evaporation cross section measured in the reaction with $^{244}$Pu.

The considerable drop of the evaporation cross sections of the $^{239}$Pu + $^{48}$Ca and $^{240}$Pu + $^{48}$Ca reactions as well as the decline of the half-life and dominance of spontaneous fission over $\alpha$ decay for $^{284}$Fl and increased growth of the $\alpha$-decay energy of $^{285}$Fl compared to the heavier Fl isotopes indicate one is approaching the neutron-deficient border of stability of SHN.

## ACKNOWLEDGMENTS

We would like to express our gratitude to the personnel of the U400 cyclotron and the associates of the ion-source group for obtaining intense $^{48}$Ca beams, V. I. Krashonkin and A. M. Zubareva for their help in performing the experiment, and V. B. Zlokazov for development of a code for the automatic spectrum calibration.

The $^{240}$Pu used in this research was partially supplied by the United States Department of Energy Office of Science by the Isotope Program in the Office of Nuclear Physics.

These studies were supported by the Russian Foundation for Basic Research, including recent Grants No. 13-02-12052 and No. 13-03-12205, and by the Moscow Region Government through Grant No. 736/36-16.09.2014. Research at ORNL was supported by the U.S. DOE Office of Nuclear Physics under DOE Contract No. DE-AC05-00OR22725 with UT-Battelle, LLC. Research at LLNL was supported by LDRD Program Project No. 08-ERD-030, under DOE Contract No. DE-AC52-07NA27344 with Lawrence Livermore National Security, LLC. This work was also supported by the U.S. DOE through Grant No. DE-FG-05-88ER40407 (Vanderbilt University).

[1] Yu. Ts. Oganessian and V. K. Utyonkov, Rep. Prog. Phys. **78**, 036301 (2015).
[2] Yu. Ts. Oganessian *et al.*, Phys. Rev. C **79**, 024603 (2009).
[3] S. Hofmann *et al.*, GSI Scientific Report 2008, GSI Report No. 2009-1, 131 (2009).
[4] S. Hofmann *et al.*, GSI Scientific Report 2011, GSI Report No. 2012-1, 205 (2012).
[5] Ch. E. Düllmann *et al.*, GSI Scientific Report 2011, GSI Report No. 2012-1, 206 (2012).
[6] S. Ćwiok, P.-H. Heenen, and W. Nazarewicz, Nature (London) **433**, 705 (2005).
[7] M. M. Sharma, A. R. Farhan, and G. Münzenberg, Phys. Rev. C **71**, 054310 (2005).
[8] A. Staszczak, A. Baran, and W. Nazarewicz, Phys. Rev. C **87**, 024320 (2013).
[9] D. Rudolph *et al.*, Phys. Rev. Lett. **111**, 112502 (2013).
[10] Yue Shi, D. E. Ward, B. G. Carlsson, J. Dobaczewski, W. Nazarewicz, I. Ragnarsson, and D. Rudolph, Phys. Rev. C **90**, 014308 (2014).
[11] V. I. Zagrebaev, Nucl. Phys. A **734**, 164 (2004).
[12] V. I. Zagrebaev and W. Greiner, Phys. Rev. C **78**, 034610 (2008).
[13] J. B. Roberto, C. W. Alexander, R. A. Boll, D. J. Dean, J. G. Ezold, L. K. Felker, and K. P. Rykaczewski, in *Proceedings of the Fifth International Conference on Fission and Properties of Neutron-Rich Nuclei, 2012*, edited by J. H. Hamilton and A. V. Ramayya (World Scientific, Singapore, 2014), p. 287.

[14] Yu. Ts. Oganessian *et al.*, Phys. Rev. C **70**, 064609 (2004).
[15] Yu. Ts. Oganessian *et al.*, Phys. Rev. C **76**, 011601(R) (2007).
[16] M. Wang, G. Audi, A. H. Wapstra, F. G. Kondev, M. MacCormick, X. Xu, and B. Pfeiffer, Chin. Phys. C **36**, 1603 (2012).
[17] W. D. Myers and W. J. Swiatecki, Nucl. Phys. A **601**, 141 (1996).
[18] Yu. Ts. Oganessian *et al.*, Phys. Rev. C **87**, 054621 (2013).
[19] K. Rykaczewski *et al.*, Nucl. Phys. A **701**, 179 (2002).
[20] R. Grzywacz, Nucl. Instrum. Methods Phys. Res., Sect. B **204**, 649 (2003).
[21] D. Miller, K. Miernik, D. Ackermann, R. Grzywacz, S. Heinz, F. P. Heßberger, S. Hofmann, J. Maurer, K. Rykaczewski, and H. Tan, GSI Scientific Report 2011, GSI Report No. 2012-1, 220 (2012).
[22] R. Grzywacz, C. J. Gross, A. Korgul, S. N. Liddick, C. Mazzocchi, R. D. Page, and K. Rykaczewski, Nucl. Instrum. Methods Phys. Res., Sect. B **261**, 1103 (2007).
[23] M. M. Rajabali *et al.*, Phys. Rev. C **85**, 034326 (2012); Mesytec GmbH & Co. KG, Multichannel Logarithmic preamplifier, http://www.mesytec.com.
[24] P. A. Ellison *et al.*, Phys. Rev. Lett. **105**, 182701 (2010).
[25] K.-H. Schmidt, C.-C. Sahm, K. Pielenz, and H.-G. Clerc, Z. Phys. A: At. Nucl. **316**, 19 (1984).
[26] N. J. Stoyer *et al.*, Nucl. Instrum. Methods Phys. Res. A **455**, 433 (2000); M. A. Stoyer *et al.*, Eur. Phys. J. A **25**, 595 (2005); M. A. Stoyer, S. Y. Strauss *et al.* (unpublished).
[27] R. N. Sagaidak, V. K. Utyonkov, and F. Scarlassara, Nucl. Instrum. Methods Phys. Res., Sect. A **700**, 111 (2013).
[28] Yu. Ts. Oganessian *et al.*, Phys. Rev. C **69**, 021601(R) (2004).
[29] Yu. Ts. Oganessian *et al.*, Phys. Rev. C **87**, 014302 (2013).
[30] *Table of Superdeformed Nuclear Bands and Fission Isomers*, 2nd ed., edited by B. Singh, R. B. Firestone, and S. Y. F. Chu (Wiley, New York, 1996); B. Singh, R. Zywina, and R. B. Firestone, Nucl. Data Sheets **97**, 241 (2002).
[31] D. C. Hoffman and M. R. Lane, Radiochim. Acta **70–71**, 135 (1995).
[32] V. I. Zagrebaev, A. V. Karpov, and W. Greiner, Phys. Rev. C **85**, 014608 (2012).
[33] G. G. Adamian, N. V. Antonenko, and W. Scheid, Phys. Rev. C **69**, 014607 (2004).
[34] Yu. Ts. Oganessian *et al.*, Phys. Rev. C **69**, 054607 (2004).
[35] J. M. Gates *et al.*, Phys. Rev. C **83**, 054618 (2011).
[36] E. M. Kozulin *et al.*, Phys. Rev. C **90**, 054608 (2014).
[37] P. Möller, J. R. Nix, W. D. Myers, and W. J. Swiatecki, At. Data Nucl. Data Tables **59**, 185 (1995).
[38] M. Kowal, P. Jachimowicz, and A. Sobiczewski, Phys. Rev. C **82**, 014303 (2010).
[39] I. Muntian, S. Hofmann, Z. Patyk, and A. Sobiczewski, Acta Phys. Pol. B **34**, 2073 (2003).
[40] I. Muntian, Z. Patyk, and A. Sobiczewski, Phys. At. Nucl. **66**, 1015 (2003).
[41] V. I. Zagrebaev, Y. Aritomo, M. G. Itkis, Yu. Ts. Oganessian, and M. Ohta, Phys. Rev. C **65**, 014607 (2001).
[42] R. Smolańczuk, J. Skalski, and A. Sobiczewski, Phys. Rev. C **52**, 1871 (1995).
[43] R. Smolańczuk, Phys. Rev. C **56**, 812 (1997).
[44] G. Audi, F. G. Kondev, M. Wang, B. Pfeiffer, X. Sun, J. Blachot, and M. MacCormick, Chin. Phys. C **36**, 1157 (2012).
[45] G. Audi, M. Wang, A. H. Wapstra, F. G. Kondev, M. MacCormick, X. Xu, and B. Pfeiffer, Chin. Phys. C **36**, 1287 (2012).